

Radiative decays of bottomonia into charmonia and light mesons

Ying-Jia Gao ^(a), Yu-Jie Zhang ^(a), and Kuang-Ta Chao ^(a)

^(a) *Department of Physics, Peking University, Beijing 100871, People's Republic of China*

In the framework of nonrelativistic QCD, we study the radiative decays of bottomonia into charmonia, including $\Upsilon \rightarrow \chi_{cJ}\gamma$, $\Upsilon \rightarrow \eta_c\gamma$, $\eta_b \rightarrow J/\psi\gamma$, and $\chi_{bJ} \rightarrow J/\psi\gamma$. We give predictions for their branching ratios with numerical calculations. E.g., we predict the branching ratio for $\eta_b \rightarrow J/\psi\gamma$ is about 1×10^{-7} . As a phenomenological model study, we further extend our calculation to the radiative decays of bottomonia into light mesons by assuming the $f_2(1270)$, $f_2'(1525)$ and other light mesons to be described by nonrelativistic $q\bar{q}$ ($q = u, d, s$) bound states with constituent quark masses. The calculated branching ratios for $\Upsilon \rightarrow f_2(1270)\gamma$ and $\Upsilon \rightarrow f_2'(1525)\gamma$ are roughly consistent with the CLEO data. Comparisons with radiative decays of charmonium into light mesons such as $J/\psi \rightarrow f_2(1270)\gamma$ are also given. In all calculations the QED contributions are taken into account and found to be significant in some processes.

PACS numbers: 12.38.Bx; 13.25.Hw; 14.40.Gx

I. INTRODUCTION

Radiative decays of bottomonium (e.g. Υ , η_b , χ_{cJ}) into charmonium are expected to be described by nonrelativistic quantum chromodynamics (NRQCD), since both bottomonium and charmonium are made of heavy quark and heavy antiquark, and are nonrelativistic bound states. For heavy quarkonium decay and production, the rates can be factorized into a short-distance part, which can be calculated in QCD perturbatively, and a long-distance part, which are governed by nonperturbative QCD dynamics [1]. Therefore, radiative decays of bottomonium into charmonium may provide a useful test for NRQCD factorization, which is assumed to hold also for these specific exclusive processes, and may also provide some practical estimates for decays such as $\eta_b \rightarrow J/\psi\gamma$, which might be useful in search for the not yet discovered η_b meson. As a phenomenological model study, we further extend our calculation to the radiative decays of bottomonia into light mesons by assuming the $f_2(1270)$, $f_2'(1525)$ and other light mesons to be described by nonrelativistic $q\bar{q}$ ($q = u, d, s$) bound states with m_q ($q = u, d$) = 350 MeV, $m_s = 500$ MeV as their constituent masses as in constituent quark models. These decays are known as the gluon rich channels, and regarded as a good place to investigate the interactions between quarks and gluons in these OZI forbidden processes, and there have been some earlier work discussing these processes (see, e.g., [2, 3]). In this paper, as our previous work [4], we will perform a complete numerical calculation for the quark-gluon loop diagrams involved in these processes, and we will also include contributions from QED diagrams.

We adopt the descriptions of nonrelativistic bound states, i.e., both heavy quarkonium and light mesons are described by the color-singlet non-relativistic wave functions. Based on this point, we studied $\Upsilon \rightarrow \chi_{cJ}\gamma$, $\Upsilon \rightarrow \eta_c\gamma$, $\Upsilon \rightarrow f_J\gamma$, $\Upsilon \rightarrow \eta\gamma$, $J/\psi \rightarrow f_J\gamma$, $J/\psi \rightarrow \eta\gamma$, $\chi_{bJ} \rightarrow J/\psi(\rho, \omega, \phi)\gamma$ and $\eta_b \rightarrow J/\psi(\rho, \omega, \phi)\gamma$ et ac. We also put this assumption into use for the glue-ball candidates such as η , η' and $f_0(1710)$, and it maybe give a clear station about these meson' components.

The structure of this paper is shown below: In section II, we will give the main techniques in our calculations, and then predict the branch ratio of $\Upsilon \rightarrow \chi_{cJ}\gamma$, $\Upsilon \rightarrow \eta_c\gamma$ and $\chi_{bJ} \rightarrow J/\psi\gamma$. Then, in the following section, we will generalize this method to those processes in which the final states are light mesons. Finally, we will summary all the results in section IV.

II. BOTTOMONIUM RADIATIVE DECAYS TO CHARMONIUM

In this section, we will study the radiative decays of bottomonium into charmonium. The decay amplitude that describe the creation of the color-singlet $c\bar{c}$ pairs, under the nonrelativistic approximation, which subsequently hadronize in Υ decays as Fig.1 shows can be expressed as[5]

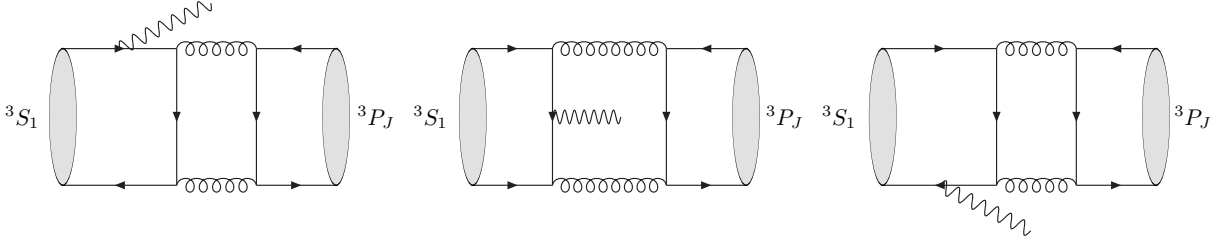


FIG. 1: Half of the Feynman diagrams of QCD process for heavy quarkonium (3S_1) radiative decays to (3P_J) mesons

$$\begin{aligned}
\mathcal{A}\left(b\bar{b}({}^3S_1)(2p_b) \rightarrow c\bar{c}({}^{2S+1}L_J)(2p_c)\right) &= \sqrt{C_{L_T}}\sqrt{C_L} \sum_{L_T z} \sum_{S_T z} \sum_{s_1 s_2} \sum_{jk} \sum_{L_z S_z} \sum_{s_3 s_4} \sum_{il} \\
&\times \langle 1 | \bar{3}k; 3j \rangle \langle J_T J_{Tz} | L_T L_{Tz}; S_T S_{Tz} \rangle \langle S_T S_{Tz} | s_1; s_2 \rangle \\
&\times \langle s_3; s_4 | SS_z \rangle \langle LL_z; SS_z | JJ_z \rangle \langle 3l; \bar{3}i | 1 \rangle \\
&\times \begin{cases} \mathcal{A}(b_j(p_b) + \bar{b}_k(p_b) \rightarrow \gamma(p_3) + c_l(p_c) + \bar{c}_i(p_c)) & (L = S), \\ \epsilon_\alpha^*(L_z) \mathcal{A}^\alpha(b_j(p_b) + \bar{b}_k(p_b) \rightarrow \gamma(p_3) + c_l(p_c) + \bar{c}_i(p_c)) & (L = P), \end{cases} \quad (1)
\end{aligned}$$

where $\langle 3l; \bar{3}i | 1 \rangle = \delta_{li}/\sqrt{N_c}$, $\langle s_1; s_2 | SS_z \rangle$, and $\langle LL_z; SS_z | JJ_z \rangle$ are respectively the color-SU(3), spin-SU(2), and angular momentum Clebsch-Gordan coefficients for $Q\bar{Q}$ pairs projecting out appropriate bound states. $\mathcal{A}(b_j(p_b) + \bar{b}_k(p_b) \rightarrow Q_l(p_c) + \bar{Q}_i(p_c))$ is the decay amplitude for $Q\bar{Q}$ production and \mathcal{A}^α is the derivative of the amplitude with respect to the relative momentum between the quark and anti-quark in the bound state. The coefficients C_{L_T} and C_L can be related to the radial wave function of the bound states or its derivative with respect to the relative spacing as

$$C_S = \frac{1}{4\pi} |R_s(0)|^2, \quad C_P = \frac{3}{4\pi} |R'_p(0)|^2. \quad (2)$$

The spin projection operators $P_{SS_z}(p, q)$ which describes the production of quarkonium are constructed in terms of quark and anti-quark spinors as[5, 6]:

$$P_{SS_z}(p, q) = \sum_{s_1, s_2} v\left(\frac{p}{2} - q, s_2\right) \bar{u}\left(\frac{p}{2} + q, s_1\right) \langle s_1; s_2 | SS_z \rangle, \quad (3)$$

We list the spin projection operators and their derivatives with respect to the relative momentum, which we will use in the calculations, as

$$P_{00}(p, 0) = \frac{1}{2\sqrt{2}} \gamma_5 (\not{p} + 2m), \quad (4)$$

$$P_{1S_z}(p, 0) = \frac{1}{2\sqrt{2}} \not{\epsilon}^*(S_z) (\not{p} + 2m), \quad (5)$$

$$P_{1S_z}^\alpha(p, 0) = \frac{1}{4\sqrt{2}m} [\gamma^\alpha \not{\epsilon}^*(S_z) (\not{p} + 2m) - (\not{p} - 2m) \not{\epsilon}^*(S_z) \gamma^\alpha]. \quad (6)$$

And the spin projection operators which describes the annihilation of quarkonium are the complex conjugate of the corresponding operators of production. The polarization relations for the 3P_J states are shown below:

$$\sum_{L_z S_z} \epsilon^{*\alpha}(L_z) \epsilon^{*\beta}(S_z) \langle 1L_z; 1S_z | 1J_z \rangle = \frac{-i\epsilon^{\alpha\beta\lambda\kappa} p_\kappa \epsilon_\lambda^*(J_z)}{\sqrt{2}M}, \quad (7)$$

$$\sum_{L_z S_z} \epsilon^{*\alpha}(L_z) \epsilon^{*\beta}(S_z) \langle 1L_z; 1S_z | 00 \rangle = \frac{1}{\sqrt{3}} \left(-g^{\alpha\beta} + \frac{p^\alpha p^\beta}{M^2}\right), \quad (8)$$

$$\sum_{L_z S_z} \epsilon^{*\alpha}(L_z) \epsilon^{*\beta}(S_z) \langle 1L_z; 1S_z | 2J_z \rangle = \epsilon^{*\alpha\beta}(J_z), \quad (9)$$

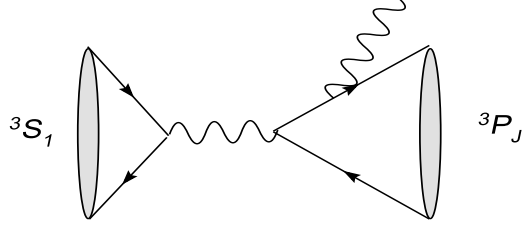


FIG. 2: Half of the Feynman diagrams of QED process for heavy quarkonium (3S_1) radiative decays to (3P_J) mesons

where p is the momentum of P-wave quarkonium, and M is the mass of the corresponding quarkonium. $\epsilon_\lambda(J_z)$ is the polarization vector of $J = 1$. $\epsilon^{\alpha\beta}(J_z)$ is the polarization vector of $J = 2$, which is symmetric under the exchange $\alpha \leftrightarrow \beta$.

The QCD Feynman diagrams of $\Upsilon \rightarrow \gamma\eta_c(\chi_{cJ})$ was shown in FIG.1. The QED Feynman diagrams was shown in FIG.2. In the calculation, we use `FeynCalc` [7] for the tensor reduction and `LoopTools`[8] for the numerical evaluation of infrared safe integrals. We follow the way in Ref.[9] to deal with five-point functions and high tensor loop integrals that can not be calculated by `LoopTools` and `FeynCalc`, such as

$$E_{\alpha\beta\rho\sigma} = \int d^Dk \frac{k_\alpha k_\beta k_\rho k_\sigma}{k^2[(k+p_c)^2 - m_c^2](k+2p_c)^2[(p_b+k)^2 - m_b^2][(k+2p_c-p_b)^2 - m_b^2]}. \quad (10)$$

where p_c is the momentum of c quark, p_b the momentum of b quark, m_c the charm quark mass, and m_b the bottom quark mass.

In the numerical calculation, the quark masses were selected as $m_b = 4.7 \text{ GeV}$, $m_c = 1.5 \text{ GeV}$, the wave functions at the origin can be found in Ref.[10], $|\mathcal{R}_S^{bb}(0)|^2 = 6.477 \text{ GeV}^3$, $|\mathcal{R}_S^{cc}(0)|^2 = 0.81 \text{ GeV}^3$, $|\mathcal{R}_P^{bb}(0)|^2 = 1.417 \text{ GeV}^5$, $|\mathcal{R}'_{c\bar{c}}(0)|^2 = 0.075 \text{ GeV}^5$. In the bottomonium decay, the strong coupling constant was select as $\alpha_s = 0.19$. The numerical result of radiative decays of bottomonium to charmonium was list in Table I.

We can estimate the total width of η_b through consider $\Gamma_{tot}(\eta_b) \approx \Gamma(\eta_b \rightarrow gg)$ [1]. To the $\Gamma(\eta_b \rightarrow gg)$,

$$\Gamma(\eta_b \rightarrow gg) = \frac{|\mathcal{R}_s(0)|^2 C_F \alpha_s^2 (2m_b)}{2m_b^2} \left\{ 1 + \left[\left(\frac{\pi^2}{4} - 5 \right) C_F + \left(\frac{199}{18} - \frac{13\pi^2}{24} \right) C_A - \frac{8}{9} n_f \right] \frac{\alpha_s}{\pi} \right\}. \quad (11)$$

In another hand, the wave function at the origin $|\mathcal{R}_s(0)|^2$ is related with leptonic width of Υ ,

$$\Gamma(\Upsilon \rightarrow e^+e^-) = N_c Q_b^2 \alpha^2 \frac{|\mathcal{R}_s(0)|^2}{3m_b^2} \left(1 - \frac{16\alpha_s}{3\pi} \right), \quad (12)$$

we can get

$$\Gamma_{tot}(\eta_b) = \frac{3C_F \alpha_s^2 (2m_b)}{2N_c Q_b^2 \alpha^2} \frac{1 + \left[\left(\frac{\pi^2}{4} - 5 \right) C_F + \left(\frac{199}{18} - \frac{13\pi^2}{24} \right) C_A - \frac{8}{9} n_f \right] \frac{\alpha_s}{\pi}}{1 - \frac{16\alpha_s}{3\pi}} \Gamma(\Upsilon \rightarrow e^+e^-). \quad (13)$$

Using $m_b = 4.7 \text{ GeV}$, $\alpha_s(2m_b) = 0.19$ and experiment data $\Gamma(\Upsilon \rightarrow e^+e^-) = 1.340 \pm 0.018 \text{ KeV}$ [13], we can get $\Gamma_{tot}(\eta_b) \approx 13.0 \text{ MeV}$. Then the branch ratios $Br(\eta_b \rightarrow \gamma J/\psi) \approx 7.3 \times 10^{-8}$. If we use the leading order formula in Eq(11) and Eq(12), the $\Gamma_{tot}(\eta_b) \approx 5.45 \text{ MeV}$, the branch ratios $Br(\eta_b \rightarrow \gamma J/\psi) \approx 1.7 \times 10^{-7}$.

We can estimate the total width of η_b through consider $\Gamma_{tot}(\eta_b) \approx \Gamma(\eta_b \rightarrow gg)$ [1]. To the $\Gamma(\eta_b \rightarrow gg)$,

$$\Gamma(\eta_b \rightarrow gg) = \frac{|\mathcal{R}_s(0)|^2 C_F \alpha_s^2 (2m_b)}{2m_b^2} \left\{ 1 + \left[\left(\frac{\pi^2}{4} - 5 \right) C_F + \left(\frac{199}{18} - \frac{13\pi^2}{24} \right) C_A - \frac{8}{9} n_f \right] \frac{\alpha_s}{\pi} \right\}. \quad (14)$$

The parameters was select as $m_b = 4.7 \text{ GeV}$, $\alpha_s(2m_b) = 0.19$ and $|\mathcal{R}_S^{bb}(0)|^2 = 6.477 \text{ GeV}^3$. We can get $\Gamma_{tot}(\eta_b) \approx 11.4 \text{ MeV}$. Then the branch ratios $Br(\eta_b \rightarrow \gamma J/\psi) \approx 8.4 \times 10^{-8}$. If we use the leading order formula in Eq(14), the $\Gamma_{tot}(\eta_b) \approx 7.1 \text{ MeV}$, the branch ratios $Br(\eta_b \rightarrow \gamma J/\psi) \approx 1.4 \times 10^{-7}$.

process	$\Upsilon \rightarrow \chi_{c2}\gamma$	$\Upsilon \rightarrow \chi_{c1}\gamma$	$\Upsilon \rightarrow \chi_{c0}\gamma$	$\Upsilon \rightarrow \eta_c\gamma$
BR_{QCD}	5.1×10^{-6}	4.5×10^{-6}	4.0×10^{-6}	2.9×10^{-5}
$BR_{QCD+QED}$	5.6×10^{-6}	9.8×10^{-6}	3.2×10^{-6}	4.9×10^{-5}
process	$\chi_{b2} \rightarrow J/\psi\gamma$	$\chi_{b1} \rightarrow J/\psi\gamma$	$\chi_{b0} \rightarrow J/\psi\gamma$	$\eta_b \rightarrow J/\psi\gamma$
$\Gamma_{QCD}(\text{GeV})$	2.7×10^{-10}	3.8×10^{-10}	5.0×10^{-10}	2.8×10^{-9}
$\Gamma_{QCD+QED}(\text{GeV})$	3.6×10^{-10}	3.7×10^{-10}	1.3×10^{-10}	9.6×10^{-10}
$\Gamma_{QED}(\text{GeV})$	3.8×10^{-11}	3.3×10^{-12}	1.3×10^{-10}	1.2×10^{-9}

TABLE I: Numerical results for radiative decays of bottomonium into charmonium

	QCD	QCD+QED		QCD	QCD+QED
$x^2(\Upsilon \rightarrow \gamma\chi_{c2})$	0.37	0.38	$x^2(\Upsilon \rightarrow \gamma\chi_{c1})$	0.064	0.075
$y^2(\Upsilon \rightarrow \gamma\chi_{c2})$	0.14	0.14			

TABLE II: Results for $\Upsilon \rightarrow \chi_{cJ}\gamma$ with different helicity states

Besides these, we also want to give the branch ratios for different helicities. As in Ref. [11], we choose the moving direction of χ_{cJ} as the z-axis, and introduce three polarization vectors:

$$\begin{aligned}
\omega^\mu(1) &= \frac{-1}{\sqrt{2}}(0, 1, i, 0), \\
\omega^\mu(-1) &= \frac{1}{\sqrt{2}}(0, 1, -i, 0) \\
\omega^\mu(0) &= \frac{1}{m}(|\mathbf{k}|, 0, 0, k^0),
\end{aligned} \tag{15}$$

thus we can characterize the tensor $\epsilon^{\mu\nu}(\lambda)$ of χ_{c2}

$$\begin{aligned}
\epsilon^{\alpha\beta}(2) &= \omega^\alpha(1)\omega^\beta(1) \\
\epsilon^{\alpha\beta}(1) &= \frac{1}{\sqrt{2}}(\omega^\alpha(1)\omega^\beta(0) + \omega^\alpha(0)\omega^\beta(1)) \\
\epsilon^{\alpha\beta}(0) &= \frac{1}{\sqrt{6}}(\omega^\alpha(-1)\omega^\beta(1) + 2\omega^\alpha(0)\omega^\beta(0) + \omega^\alpha(1)\omega^\beta(-1)) \\
\epsilon^{\alpha\beta}(-1) &= \frac{1}{\sqrt{2}}(\omega^\alpha(0)\omega^\beta(-1) + \omega^\alpha(-1)\omega^\beta(0)) \\
\epsilon^{\alpha\beta}(-2) &= \omega^\alpha(-1)\omega^\beta(-1)
\end{aligned} \tag{16}$$

Consistent with the experiment date, the helicity production ratios were introduced as

$$x^2 = \frac{|a_1|^2}{|a_0|^2} \text{ and } y^2 = \frac{|a_2|^2}{|a_0|^2},$$

where a_λ , $\lambda = 0, 1, 2$, are the normalized helicity amplitudes, which satisfy $|a_0|^2 + |a_1|^2 + |a_2|^2 = 1$. In other words, $|a_\lambda|^2$ is the probability of final meson in helicity $\pm\lambda$ states. Then ratios x^2 and y^2 only depend on the ratio of mass m_c/m_b . With the same choosing of parameters, we give ratios for different helicities in Table II.

III. HEAVY QUARKONIUM INTO LIGHT MESONS

In the numerical calculation, the light quark masses were selected as $m_s = 0.50 \text{ GeV}$, $m_u = m_d = 0.35 \text{ GeV}$. The parameters about heavy quark are same with that were used in section II, $|\mathcal{R}_S^{bb}(0)|^2 = 6.477 \text{ GeV}^3$, $|\mathcal{R}_S^{c\bar{c}}(0)|^2 = 0.81 \text{ GeV}^3$, $|\mathcal{R}_P^{bb}(0)|^2 = 1.417 \text{ GeV}^5$, $|\mathcal{R}_P^{c\bar{c}}(0)|^2 = 0.075 \text{ GeV}^5$, $m_b = 4.7 \text{ GeV}$, and $m_c = 1.5 \text{ GeV}$. The strong coupling constant was select as $\alpha_s = 0.19$ and $\alpha_s = 0.26$ in bottomonium and charmonium decay respectively.

As widely accepted assignments we assume that $f_2(1270)$ and $f_1(1285)$ are mainly composed of $(u\bar{u} + d\bar{d})/\sqrt{2}$ (neglecting the mixing with $s\bar{s}$ for simplicity). But for $f_0(980)$, there are many possible assignments such as the tetraquark state, the $K\bar{K}$ molecule, and the P-wave $s\bar{s}$ dominated state (for related discussions on $f_0(980)$ and other

scalar mesons, see, e.g., the topical review–note on scalar mesons in [13] and [14]). Since experimental data show that $D_s^+ \rightarrow f_0\pi^+$ has a large branching ratio (BR)[13], we prefer to assign $f_0(980)$ as an $s\bar{s}$ dominated P-wave state as a tentative choice.

As to the wave function at the origin of light mesons, it is very difficult to determine them without doubt. Using the theoretical expression for the widths of $f_2 \rightarrow \gamma\gamma$ [1],

$$\begin{aligned}\Gamma_{f_2(1270) \rightarrow \gamma\gamma}^{(th)} &= \frac{6N_c}{5}(Q_u^2 + Q_d^2)^2 \alpha^2 \frac{|\mathcal{R}'_P(0)|^2}{m^4} \left(1 - \frac{8\alpha_s}{3\pi}\right)^2 \\ \Gamma_{f_2'(1525) \rightarrow \gamma\gamma}^{(th)} &= \frac{12N_c}{5} Q_s^4 \alpha^2 \frac{|\mathcal{R}'_P(0)|^2}{m^4} \left(1 - \frac{8\alpha_s}{3\pi}\right)^2,\end{aligned}\quad (17)$$

where $N_c=3$ is the color number, $\alpha = 1/137$, and fitting them with their experimental values 2.6 KeV and 0.081 KeV for $f_2(1270)$ and $f_2'(1525)$ respectively[13], we get

$$\begin{aligned}|\mathcal{R}'_P^{m\bar{n}}(0)|^2 &= 1.58 \times 10^{-3} \text{ GeV}^5, \\ |\mathcal{R}'_P^{s\bar{s}}(0)|^2 &= 2.23 \times 10^{-3} \text{ GeV}^5.\end{aligned}\quad (18)$$

If we use leading order formula in Eq(17), then

$$\begin{aligned}|\mathcal{R}_P^{m\bar{n}}(0)|^2 &= 6.6 \times 10^{-4} \text{ GeV}^5 \\ |\mathcal{R}_P^{s\bar{s}}(0)|^2 &= 1.1 \times 10^{-3} \text{ GeV}^5.\end{aligned}\quad (19)$$

For the vector mesons, the wave function at the origin may be determined from their leptonic decay $V \rightarrow e^+e^-$ ($V = \phi, \rho$). Using

$$\Gamma(\phi(1020) \rightarrow e^+e^-) = N_c Q_s^2 \alpha^2 \frac{|\mathcal{R}(0)|^2}{3m_s^2} \left(1 - \frac{8\alpha_s}{3\pi}\right)^2 = (1.27 \pm 0.04) \text{ KeV},\quad (20)$$

We can get

$$\begin{aligned}|\mathcal{R}_S^{n\bar{n}}(0)|^2 &= 0.11 \text{ GeV}^3, \\ |\mathcal{R}_S^{s\bar{s}}(0)|^2 &= 0.19 \text{ GeV}^3.\end{aligned}\quad (21)$$

If we use leading order formula in Eq(20), then

$$\begin{aligned}|\mathcal{R}_S^{n\bar{n}}(0)|^2 &= 0.032 \text{ GeV}^3, \\ |\mathcal{R}_S^{s\bar{s}}(0)|^2 &= 0.054 \text{ GeV}^3.\end{aligned}\quad (22)$$

As to the wave function at the origin of light mesons, it can be determined from potential model [15]. From experiment data, $\Delta E = M(2S) - M(1S)$ is 675 MeV, 638 MeV, 661 MeV, 589 MeV, and 563 MeV for $\rho, \omega, \phi, J/\psi$, and Υ respectively. In the logarithmic potential, ΔE is independent on quark mass. So that we select logarithmic potential. In the logarithmic potential,

$$\begin{aligned}|R_S(0)|^2 &\propto m_q^{3/2} \\ |R_P(0)|^2 &\propto m_q^{5/2}\end{aligned}\quad (23)$$

With $|\mathcal{R}_S^{c\bar{c}}(0)|^2 = 0.81 \text{ GeV}^3$ and $|\mathcal{R}'_P^{c\bar{c}}(0)|^2 = 0.075 \text{ GeV}^5$ ¹. Then we can get

$$\begin{aligned}|\mathcal{R}_S^{n\bar{n}}(0)|^2 &= \left(\frac{m_n}{m_c}\right)^{3/2} |\mathcal{R}_S^{c\bar{c}}(0)|^2 = 0.091 \text{ GeV}^3 \\ |\mathcal{R}_S^{s\bar{s}}(0)|^2 &= \left(\frac{m_s}{m_c}\right)^{3/2} |\mathcal{R}_S^{c\bar{c}}(0)|^2 = 0.156 \text{ GeV}^3 \\ |\mathcal{R}'_P^{m\bar{n}}(0)|^2 &= \left(\frac{m_n}{m_c}\right)^{5/2} |\mathcal{R}'_P^{c\bar{c}}(0)|^2 = 1.97 \times 10^{-3} \text{ GeV}^5 \\ |\mathcal{R}'_P^{s\bar{s}}(0)|^2 &= \left(\frac{m_s}{m_c}\right)^{5/2} |\mathcal{R}'_P^{c\bar{c}}(0)|^2 = 4.81 \times 10^{-3} \text{ GeV}^5\end{aligned}\quad (24)$$

¹ The wavefunction at origin in logarithmic potential for $c\bar{c}$ is $|\mathcal{R}_S^{c\bar{c}}(0)|^2 = 0.815 \text{ GeV}^3$ and $|\mathcal{R}'_P^{c\bar{c}}(0)|^2 = 0.078 \text{ GeV}^5$. It is consistent with the B-T potential result that was used here.

process	$\Upsilon \rightarrow \gamma f_0(n\bar{n})$	$\Upsilon \rightarrow \gamma f_1(1285)$	$\Upsilon \rightarrow \gamma f_2(1270)$	$\Upsilon \rightarrow \gamma f_0(980)$	$\Upsilon \rightarrow \gamma f'_1(1420)$	$\Upsilon \rightarrow \gamma f'_2(1525)$
BR_{th}^{QCD}	7.2×10^{-5}	2.6×10^{-5}	7.1×10^{-5}	2.2×10^{-5}	1.0×10^{-5}	2.2×10^{-5}
$BR_{th}^{QCD+QED}$	6.4×10^{-5}	3.9×10^{-5}	6.3×10^{-5}	2.0×10^{-5}	1.2×10^{-5}	2.0×10^{-5}
BR_{ex}	\	\	$1.00 \pm 0.10 \times 10^{-4}$	$< 3 \times 10^{-5}$	\	$3.7_{-1.1}^{+1.2} \times 10^{-5}$
process	$J/\psi \rightarrow \gamma f_0(n\bar{n})$	$J/\psi \rightarrow \gamma f_1(1285)$	$J/\psi \rightarrow \gamma f_2(1270)$	$J/\psi \rightarrow \gamma f_0(980)$	$J/\psi \rightarrow \gamma f'_1(1420)$	$J/\psi \rightarrow \gamma f'_2(1525)$
BR_{th}^{QCD}	2.0×10^{-3}	2.0×10^{-3}	2.5×10^{-3}	6.7×10^{-4}	7.5×10^{-4}	8.5×10^{-4}
$BR_{th}^{QCD+QED}$	1.8×10^{-3}	2.7×10^{-3}	2.4×10^{-3}	6.5×10^{-4}	8.5×10^{-4}	8.5×10^{-4}
BR_{ex}	\	$(6.1 \pm 0.8) \times 10^{-4}$	$(13.8 \pm 1.4) \times 10^{-4}$	\	$(7.9 \pm 1.3) \times 10^{-4}$	$(4.5_{-0.4}^{+0.7}) \times 10^{-4}$

TABLE III: Numerical results for $\Upsilon(J/\psi) \rightarrow \gamma f_J$.

process	$\chi_{b2} \rightarrow \gamma \rho$	$\chi_{b1} \rightarrow \gamma \rho$	$\chi_{b0} \rightarrow \gamma \rho$	$\eta_b \rightarrow \gamma \rho$
$\Gamma_{QCD}(\text{GeV})$	1.1×10^{-10}	2.2×10^{-10}	3.5×10^{-11}	1.2×10^{-10}
$\Gamma_{QCD+QED}(\text{GeV})$	6.8×10^{-10}	2.2×10^{-10}	8.4×10^{-10}	1.1×10^{-8}
process	$\chi_{b2} \rightarrow \gamma \omega$	$\chi_{b1} \rightarrow \gamma \omega$	$\chi_{b0} \rightarrow \gamma \omega$	$\eta_b \rightarrow \gamma \omega$
$\Gamma_{QCD}(\text{GeV})$	1.2×10^{-11}	2.4×10^{-11}	3.8×10^{-12}	1.3×10^{-11}
$\Gamma_{QCD+QED}(\text{GeV})$	7.6×10^{-11}	2.4×10^{-11}	9.3×10^{-11}	1.2×10^{-9}
process	$\chi_{b2} \rightarrow \gamma \phi$	$\chi_{b1} \rightarrow \gamma \phi$	$\chi_{b0} \rightarrow \gamma \phi$	$\eta_b \rightarrow \gamma \phi$
$\Gamma_{QCD}(\text{GeV})$	3.6×10^{-11}	5.8×10^{-11}	1.6×10^{-11}	5.9×10^{-11}
$\Gamma_{QCD+QED}(\text{GeV})$	1.3×10^{-10}	5.8×10^{-11}	7.5×10^{-11}	1.2×10^{-9}
process	$\chi_{c2} \rightarrow \gamma \rho$	$\chi_{c1} \rightarrow \gamma \rho$	$\chi_{c0} \rightarrow \gamma \rho$	$\eta_c \rightarrow \gamma \rho$
BR_{th}^{QCD}	1.3×10^{-5}	4.1×10^{-5}	3.2×10^{-6}	1.5×10^{-6}
$BR_{th}^{QCD+QED}$	3.8×10^{-5}	4.2×10^{-5}	2.0×10^{-6}	4.5×10^{-6}
process	$\chi_{c2} \rightarrow \gamma \omega$	$\chi_{c1} \rightarrow \gamma \omega$	$\chi_{c0} \rightarrow \gamma \omega$	$\eta_c \rightarrow \gamma \omega$
BR_{th}^{QCD}	1.5×10^{-6}	4.6×10^{-6}	3.5×10^{-7}	1.7×10^{-7}
$BR_{th}^{QCD+QED}$	4.2×10^{-6}	4.7×10^{-6}	2.2×10^{-7}	5.0×10^{-7}
process	$\chi_{c2} \rightarrow \gamma \phi$	$\chi_{c1} \rightarrow \gamma \phi$	$\chi_{c0} \rightarrow \gamma \phi$	$\eta_c \rightarrow \gamma \phi$
BR_{th}^{QCD}	3.3×10^{-6}	1.1×10^{-5}	1.3×10^{-6}	7.1×10^{-7}
$BR_{th}^{QCD+QED}$	6.5×10^{-6}	1.1×10^{-5}	3.0×10^{-8}	4.0×10^{-7}

TABLE IV: Predicted decay widths for $\chi_{bJ}(\eta_b) \rightarrow \gamma \rho(\omega, \phi)$.

In the numerical calculation, the parameters were selected as $|\mathcal{R}_S^{s\bar{s}}(0)|^2 = 0.054 \text{ GeV}^3$, $|\mathcal{R}_S^{n\bar{n}}(0)|^2 = 0.032 \text{ GeV}^3$, $|\mathcal{R}_P^{s\bar{s}}(0)|^2 = 1.1 \times 10^{-3} \text{ GeV}^5$, $|\mathcal{R}_P^{n\bar{n}}(0)|^2 = 6.6 \times 10^{-4} \text{ GeV}^5$. The numerical results were shown in Table III and Table IV.

The branching ratio of Υ radiative decays into a light meson is small than the correspond rate of J/ψ by a factor

$$\frac{BR(\Upsilon \rightarrow \gamma M)}{BR(J/\psi \rightarrow \gamma M)} \sim \left(\frac{Q_b}{Q_c}\right)^2 \left(\frac{m_c}{m_b}\right)^2 \frac{\alpha(2m_b)}{\alpha(2m_c)} \sim 0.02 \quad (25)$$

We can find the theoretical ratio is $0.013 \sim 0.036$. But the experiment ratio 0.072 for $f_2(1270)$, and 0.082 for $f'_2(1525)$. The corresponding theoretical ratio are 0.026 and 0.024 for $f_2(1270)$ and $f'_2(1525)$ respectively. If we use a larger constituent quark mass, e.g. $m_u = m_d = M(1270)/2$, $m_s = M(1525)/2$, the ratio are 0.018 and 0.018 for $f_2(1270)$ and $f'_2(1525)$ respectively.

With the same parameters, we give the branching ratios for different helicity states in Table V. The corresponding values of helicity parameters x and y are $x = 0.46$, $y = 0.23$. Recently, new experimental data for the contributions of different helicities in process $J/\psi \rightarrow \gamma f_2(1270)$ have been given by the BES Collaboration [?]: $x = 0.89 \pm 0.02 \pm 0.10$ and $y = 0.46 \pm 0.02 \pm 0.17$ (see also[13]). It is about 2 times larger than our results. But if we use a larger constituent quark mass, e.g. $m_u = M(1270)/2$, we will get substantially increased values $x = 0.79$ and $y = 0.58$ (also see Ref.[2]). We emphasize that the helicity parameters are very sensitive to the light quark masses, and hence very useful in clarifying the decay mechanisms. Note that if $m_u/m_c \rightarrow 0$, we will have $x \rightarrow 0$ and $y \rightarrow 0$, but this is inconsistent with data.

$m_q(\text{GeV})$		QCD	QCD+QED		QCD	QCD+QED		QCD	QCD+QED
0.35	$x^2(\Upsilon \rightarrow \gamma f_2)$	0.023	0.023	$y^2(\Upsilon \rightarrow \gamma f_2)$	0.0013	0.0014	$x^2(\Upsilon \rightarrow \gamma f_1)$	0.00069	0.00010
0.635	$x^2(\Upsilon \rightarrow \gamma f_2)$	0.073	0.075	$y^2(\Upsilon \rightarrow \gamma f_2)$	0.0095	0.010	$x^2(\Upsilon \rightarrow \gamma f_1)$	0.0047	0.0067
0.50	$x^2(\Upsilon \rightarrow \gamma f'_2)$	0.045	0.046	$y^2(\Upsilon \rightarrow \gamma f'_2)$	0.0043	0.0045	$x^2(\Upsilon \rightarrow \gamma f'_1)$	0.0018	0.0023
0.763	$x^2(\Upsilon \rightarrow \gamma f'_2)$	0.10	0.11	$y^2(\Upsilon \rightarrow \gamma f'_2)$	0.017	0.018	$x^2(\Upsilon \rightarrow \gamma f'_1)$	0.0087	0.010
0.35	$x^2(J/\psi \rightarrow \gamma f_2)$	0.21	0.21	$y^2(J/\psi \rightarrow \gamma f_2)$	0.055	0.057	$x^2(J/\psi \rightarrow \gamma f_1)$	0.026	0.029
0.635	$x^2(J/\psi \rightarrow \gamma f_2)$	0.62	0.62	$y^2(J/\psi \rightarrow \gamma f_2)$	0.33	0.33	$x^2(J/\psi \rightarrow \gamma f_1)$	0.13	0.14
0.50	$x^2(J/\psi \rightarrow \gamma f'_2)$	0.40	0.40	$y^2(J/\psi \rightarrow \gamma f'_2)$	0.16	0.16	$x^2(J/\psi \rightarrow \gamma f'_1)$	0.072	0.074
0.763	$x^2(J/\psi \rightarrow \gamma f'_2)$	0.86	0.86	$y^2(J/\psi \rightarrow \gamma f'_2)$	0.57	0.57	$x^2(J/\psi \rightarrow \gamma f'_1)$	0.21	0.22

TABLE V: Results for $\Upsilon \rightarrow \chi_{cJ}\gamma$ with different helicity states

IV. SUMMARY

In this paper, we first investigate the radiative decays of bottomonium into charmonium, such as: $\Upsilon \rightarrow \chi_{cJ}\gamma$, $\chi_{bJ} \rightarrow J/\psi\gamma$, $\eta_b \rightarrow J/\psi\gamma$ and $\Upsilon \rightarrow \eta_c\gamma$ et ac. Based on our numerical calculations, we predict that the branching ratios of $\Upsilon \rightarrow \chi_{cJ}\gamma$ and decay widths of $\chi_{bJ} \rightarrow J/\psi\gamma$. All the above processes are perturbative calculable, and we think it is a good way to test perturbative QCD.

At the next step, we focus on the cases of heavy quarkonium into light mesons, including $\Upsilon(J/\psi) \rightarrow f_J\gamma$ and $\chi_{bJ} \rightarrow \rho(\omega, \phi)\gamma$ et ac. For the former case, all the theoretical calculations fit the experimental data well. As the latter case, we just predict their widths to be checked by the new experiment.

During these work, we find some interesting things, that is the effects of QED process. For $\Upsilon \rightarrow \gamma\chi_{cJ}$ decay, pure electromagnetism process affects the final results($J = 0, 2$) a little, but for the $J = 1$ state, the result may change with a factor of 2. The same results will be seen in the decays of $\Upsilon \rightarrow \gamma f_J$ and $J/\psi \rightarrow \gamma f_J$. As the cases of χ_{bJ} decays, especially for the process $\chi_{bJ} \rightarrow \rho(\omega, \phi)\gamma$, QED process may give a dominant contribution. These effects need more attention.

We also pay some attention to the light mesons such as $\eta^{(\prime)}$ and $f_0(1710)$ which are regarded as the main candidates of glue-ball(well we don't show our results above). Although Υ radiative decays provide us a gluon rich environment, the branching ratios are all very small. This fact maybe prove the assumption that these mesons are mainly composed by quark components to be wrong.

Acknowledgments

We would like to thank Ce Meng for valuable discussions. This work was supported in part by the National Natural Science Foundation of China , and the Key Grant Project of Chinese Ministry of Education.

-
- [1] G. T. Bodwin, E. Braaten and G. P. Lepage, Phys. Rev. D **51** , 1125 (1995); **55**, 5853(E) (1997).
 - [2] J.G. Körner, J.H. Kühn, and H. Schneider, Phys. Lett. B **120**, 444 (1983); J.G. Körner , J.H. Kühn, M. Krammer, and H. Schneider, Nucl. Phys. B **229**, 115 (1983).
 - [3] M. Krammer, *Phys. Lett. B* **74**, 361 (1978); J.G. Korner and M. Krammer, *Z. Phys. C* **16**, 279 (1983).
 - [4] Y.J. Gao, Y.J. Zhang and K.T. Chao, *Chin. Phys. Lett.* **23**, 2376 (2003) (hep-ph/0607278).
 - [5] P. Cho and A.K. Leibovich, *Phys. Rev.* **D53**, 150 (1996); **53**, 6203 (1996); P. Ko, J. Lee and H.S. Song, *Phys. Rev.* **D54**, 4312 (1996); K.Y. Liu, Z.G. He, K.T. Chao, *Phys. Lett. B* **557**, 45 (2003) .
 - [6] J. H. Kühn, *Nucl. Phys. B* **157**, 125 (1979); B. Guberina *et al.*, *Nucl. Phys. B* **174**, 317 (1980).
 - [7] R. Mertig, M. Böhm, A. Denner, *Comput. Phys. Commun.* **64** (1991) 345.
 - [8] T. Hahn, M. Perez-Victoria, *Comput. Phys. Commun.* **118** (1999) 153.
 - [9] A. Denner, S. Dittmaier, *Nucl.Phys. B* **658** (2003) 175; A. Denner, S. Dittmaier, hep-ph/0509141.
 - [10] E.J. Eichten and C. Quigg, *Phys. Rev. D* **52**, 1726 (1995).
 - [11] J.P. Ma, *Nucl. Phys. B* **605** 625 (2001); Erratum-ibid. **B611** 523(2001).
 - [12] S. B. Athar *et al.* [CLEO Collaboration], *Phys. Rev. D* **73**, 032001 (2006) [arXiv:hep-ex/0510015].
 - [13] S. Eidelman, *et al.* [Particle Data Group], *Phys. Lett. B* **592** (2004) 1; W. M. Yao *et al.* [Particle Data Group], *J. Phys. G* **33**, 1 (2006).
 - [14] F.E. Close, G.R. Farrar, and Z.P. Li, *Phys. Rev. D* **55**, 5749 (1997).
 - [15] C. Quigg and J. L. Rosner, *Phys. Rept.* **56**, 167 (1979).